Redox Biology 20 (2019) 236–246

Contents lists available at ScienceDirect

Redox Biology

journal homepage: www.elsevier.com/locate/redox

Dihomo-γ-linolenic acid inhibits growth of xenograft tumors in mice bearing human pancreatic cancer cells (BxPC-3) transfected with delta-5-desaturase shRNA

Xiaoyu Yang[a], Yi Xu[a], Di Gao[a], Liu Yang[b], Steven Y. Qian[a,*]

[a] Department of Pharmaceutical Sciences, North Dakota State University, Fargo, ND 58108, USA
[b] Department of Transplantation, Mayo Clinic Florida, Jacksonville, FL 32224, USA

ARTICLE INFO

Keywords:
COX-2 catalyzed DGLA peroxidation
Delta-5-desaturase knockdown
Pancreatic cancer growth and migration
Xenograft tumor

ABSTRACT

We recently reported that siRNA-knockdown of delta-5-desaturase (D5D), the rate-limiting enzyme converting upstream ω − 6 dihomo-γ-linolenic acid (DGLA) to arachidonic acid, promoted formation of the anti-cancer byproduct 8-hydroxyoctanoic acid (8-HOA) from COX-2-catalyzed DGLA peroxidation, consequently suppressing pancreatic cancer cell growth, migration and invasion. In this study, we have further investigated the anti-tumor effects of D5D-knockdown and the resulting intensified COX-2-catalyzed DGLA peroxidation in subcutaneous xenograft tumors. Four-week old female nude mice (Jackson Laboratory, J:Nu-007850) were injected with human pancreatic cancer cell line BxPC-3 or its D5D knockdown counterpart (*via* shRNA), followed by 4-week treatments of: vehicle control, DGLA supplementation (8 mg/mouse, twice a week), gemcitabine (30 mg/kg, twice a week), and a combination of DGLA and gemcitabine. In D5D-knockdown tumors, DGLA supplementation promoted 8-HOA formation to a threshold level (> 0.3 μg/g) and resulted in significant tumor reduction (30% *vs.* control). The promoted 8-HOA not only induced apoptosis associated with altered expression of Bcl-2, cleaved PARP, procaspase 3 and procaspase 9, but also suppressed the tumor metastatic potential *via* altering MMP-2 and E-cadherin expression. DGLA supplementation resulted in similar anti-tumor effects to those of gemcitabine in our experiments, while the combined treatment led to most significant inhibitory effect on D5D-knockdown tumor growth (70% reduction *vs.* control). Compared to conventional COX-2 inhibition in cancer treatment, our new strategy that takes advantage of overexpressed COX-2 in cancer cells and tumors, and of abundant ω − 6 fatty acids in the daily diet, should lead us to develop a better and safer anti-pancreatic cancer therapy for patients.

1. Introduction

Pancreatic cancer is one of the most aggressive malignancies in the United States. There is currently no cure for pancreatic cancer as it is hard to detect at early stage, usually not treatable by surgery and radiation, and resistant to chemotherapy drugs. A variety of pharmacological and diet care regimens have been investigated as complementary strategies to improve efficacy of the standard chemotherapy for pancreatic cancer [1–8]. For example, ω-3 fatty acids including eicosapentaenoic acid and docosahexaenoic acid (mainly from marine products) have been tested in order to improve the efficacy and safety of chemotherapy [9,10]. Although ω-6s are the more abundant fatty acids in our daily diet (in traditional western diets, the ω-6 to ω-3 ratio is between ~ 10:1 and 30:1 [11–13]), ω-6-based dietary strategies have not received much attention and have been challenging in cancer treatment because deleterious metabolites can be formed from arachidonic acid (AA, a downstream ω-6 fatty acid) *via* Cyclooxygenase 2 (COX-2)-catalyzed peroxidation [14–16].

COX is a bi-functional lipid-peroxidizing enzyme that metabolizes ω-3 and ω-6 fatty acids to produce various lipid-derived molecules, including the pro-cancer metabolite prostaglandin E2 (PGE2) [14–19]. There are two isoforms of COX: COX-1, the constitutive form, which is expressed in most tissues, and COX-2, the inducible form, which can be readily induced in response to various stimuli including stresses, cytokines, growth factors, and pro-inflammatory signals as well as cancer promoters [20–22]. High COX-2 expression has been commonly found

Abbreviations: AA, arachidonic acid; COX, Cyclooxygenase; DGLA, dihomo-γ-linolenic acid; D5D, delta-5-desaturase; D5D-*KD*, delta-5-desaturase knockdown; HDAC, histone deacetylase; PGE2, prostaglandin E2; *wt*-D5D, wild type D5D; 8-HOA, 8-hydroxyoctanoic acid

* Correspondence to: Department of Pharmaceutical Science, North Dakota State University, Fargo, ND 58105, USA.
E-mail address: steven.qian@ndsu.edu (S.Y. Qian).

https://doi.org/10.1016/j.redox.2018.10.001
Received 29 August 2018; Received in revised form 18 September 2018; Accepted 2 October 2018
Available online 15 October 2018

in a variety of cancers, with over 70% of pancreatic cancer patients having been reported to possess overexpressed COX-2 [23]. A variety of COX-2 inhibitors, aiming to limit PGE2 formation from COX-2-catalyzed AA peroxidation, have been tested as a complementary strategy to enhance the efficacy of front-line chemotherapeutic drugs for pancreatic cancer treatment [24–28]. However, over the past decades, COX-2 inhibitors have never achieved the desired anti-cancer effects in clinical trials. COX-2 inhibitors not only failed to increase the survival indices of cancer patients, but also suffer from some safety issues in patients, *e.g.,* increased risks of cardiovascular disease and gastrointestinal tract injury [29–32].

Our lab recently discovered that COX-2-catalyzed DGLA peroxidation can produce the novel anti-cancer byproduct 8-hydroxyoctanoic acid (8-HOA), which can serve as a histone deacetylase inhibitor (HDACi) to inhibit cancer cell growth and metastasis in pancreatic cancer cells, *e.g.*, BxPC-3 [33–38]. However, the formation of 8-HOA from COX-catalyzed DGLA peroxidation can be limited by delta-5 desaturase (the rate-limiting enzyme to convert DGLA to AA). Thus, we previously used siRNA transfection to knock down D5D in pancreatic cancer cells *in vitro* to promote formation of 8-HOA from COX-2-catalyzed DGLA peroxidation, which in turn suppressed pancreatic cancer cell growth, migration and invasion [36,37].

In this study, we extend our strategy to *in vivo* studies confirming that D5D knockdown and DGLA supplementation can also promote the formation of 8-HOA to a threshold level in D5D-*KD* tumors, and thus significantly inhibited tumor growth and metastatic potential. In addition, concurrent DGLA supplementation along with D5D-*KD* also significantly improved the efficacy of gemcitabine in suppressing pancreatic cancer growth and metastasis. In conclusion, our new strategy of making use of the hallmark of cancer cells (*i.e.*, the commonly overexpressed COX-2) for anti-cancer purpose challenges the conventional concept of COX-2 inhibition in cancer treatment and shifts the paradigm of COX-2 cancer biology.

2. Materials and methods

2.1. Chemicals and reagents

CelLytic™ lysis reagent was obtained from Sigma-Aldrich (MO, USA). DGLA was purchased from Nu-Chek-Prep (MN, USA). Analytic standard solutions of DGLA, AA, PGE2, DGLA-d_6, AA-d_8, PGE2-d_9, and DGLA ethyl ester for animal treatment as well as gemcitabine were purchased from Cayman Chemicals (MI, USA). Pierce ECL western blot substrates were obtained from Thermo Fisher Scientific (MA, USA). X-ray film was purchased from Phoenix Research Products (NC, USA). Primary antibodies for immunofluorescence study (COX-2 (Cat# ab15191, rabbit polyclonal), D5D (Cat# ab126706, rabbit monoclonal), MMP-2 (Cat# ab37150, rabbit polyclonal), E-cadherin (Cat# ab76055, mouse monoclonal), cleaved PARP (Cat# ab32064, rabbit monoclonal), and Ki-67 (Cat# ab15880, rabbit polyclonal)) were acquired from Abcam (MA, USA). All the antibodies are validated in multiple published references; this information can be found in the corresponding product pages. CF633 goat anti-rabbit IgG(H + L) (Cat# 20122) and CF633 goat anti-mouse IgG(H + L) (Cat# 20120) were purchased from Biotium (CA, USA). Primary antibodies for western blot (bcl-2) (Cat# 4223, rabbit monoclonal), procaspase 3 (Cat# 9662, rabbit polyclonal), procaspase 9 (Cat# 9502, rabbit polyclonal), acetyl histone H3 (Cat# 9649, rabbit monoclonal), β-actin (Cat# 4970, rabbit monoclonal), and horseradish peroxidase-conjugated anti-rabbit IgG (Cat# 7074) were bought from Cell Signaling (MA, USA). D5D primary antibody (Cat# SAB2100744, rabbit polyclonal) was obtained from Sigma-Aldrich. γH2AX primary antibody (Cat# A300-081A, rabbit polyclonal) was purchased from Bethyl Laboratories (TX, USA).

DNA oligos encoding D5D-targeted shRNA with a sequence of TGCTGTAATCATCCA-GGCCAAGTCCAGTTTTGGCCACTGACTGACTGG ACTTGCTGGATGATTA (top strand) and CCTGTAATCATCCAGCAAGT CCAGTCAGTCAGTCAGTGGCCAAAACTGGACTTG-GCCTGGATGAT TAC (bottom strand) were designed (using BLOCK-IT™ RNAi Designer, www.invitrogen.com/rnai) and obtained from Integrated DNA Technologies (IA, USA). pcDNA™ 6.2-GW/EmGFP-miR vector was purchased from Invitrogen (NY, USA).

2.2. Cancer cell lines

The human pancreatic cancer cell line BxPC-3 was grown in RPMI-1640 medium (Thermo Fisher Scientific, UT, USA), supplemented with 10% fetal bovine serum (Thermo Fisher Scientific, UT, USA). Cells were cultured in an incubator containing a 95% humidified atmosphere with 5% CO_2 at 37 °C.

BxPC-3 cells were transfected with D5D shRNA to create a stable D5D knockdown cell line. The DNA oligos encoding D5D-targeted shRNA were cloned into pcDNA™ 6.2-GW/EmGFP-miR vector and transformed into *E. coli*. The shRNA-expressed vector was extracted and transfected into cells using X-tremeGENE HP DNA Transfection Reagent (Roche). A stable D5D knockdown BxPC-3 cell line was selected using blasticidin, which was later used for assessing cancer cell growth upon different treatments (*e.g.,* DGLA and gemcitabine) and developing tumor xenografts in mice.

2.3. Mouse xenograft tumor model and treatment

A total of 48 four-week old female nude mice (J:Nu, stock number 007850) were purchased from The Jackson Laboratory (Bar Harbor, ME). The mice were housed five per cage in a pathogen-free Innovive IVC system with water and food *ad libitum*. All the animal experiments were approved by the Institutional Animal Care and Use Committees at North Dakota State University. The mice were allowed to acclimatize for one week, then received subcutaneous injections of 2×10^6 *wt*-D5D and D5D-*KD* (shRNA) BxPC-3 cells (suspended in 100 μL serum-free medium) into the hind flank. The mice were fed a standard diet for another two weeks to allow the tumors to grow to a certain size, and further divided into four sub-groups for four-week treatments (6 mice per group): (1) vehicle control; (2) DGLA ethyl ester at a dose of 8 mg/mouse, oral gavage, twice a week; (3) gemcitabine at 30 mg/kg, *i.v.* injection, twice a week; and (4) both DGLA ethyl ester and gemcitabine.

Tumor growth was monitored twice a week by measuring two axes of the tumor (L, longest axis; W, shortest axis) with a digital caliper during the treatment. Tumor volume was calculated as: $V = L \times W^2/2$. At the endpoint, the mice were euthanized with an overdose of pentobarbital (200 mg/kg, *i.p.*) and the tumor tissues were collected for further analysis.

2.4. Colony formation assay

Cell survival response upon treatment with DGLA, gemcitabine, and their combination was assessed by colony formation assay. Briefly, *wt*-D5D cells and D5D-*KD* cells were seeded at 1000 cells per well into 6-well plates, and then exposed to 48 h of treatment with DGLA, gemcitabine, or their combination. The cells were then washed with PBS and incubated with fresh medium for another 10 days. After incubation, the cells were washed with PBS, fixed with 10% neutral buffered formalin, and stained with 0.05% crystal violet solution. Cell colonies formed in each well were counted using microscopy, and plate efficiency was calculated as number of colonies divided by number of cells seeded. The surviving cell fraction was calculated as the plate efficiency of the treatment group *vs.* the plate efficiency of vehicle control groups.

2.5. Cell apoptosis assay

Cell apoptosis of *wt*-D5D and D5D-*KD* BxPC-3 cells upon treatment with DGLA, gemcitabine, and their combination, was analyzed using the Annexin V Apoptosis Detection Kit I (BD Pharmingen™, NJ, USA)

according to the manufacturer's instruction. Briefly, 3.0×10^5 *wt*-D5D cells and D5D-*KD* cells were seeded overnight in each well of a 6-well plate and exposed to various treatments. Then the cells were harvested by trypsinization, washed with PBS and re-suspended in 1× binding buffer at a concentration of 1.0×10^6 cells/mL. 100 μL of such a cell suspension was treated with 5.0 μL each of FITC Annexin V and PI solution, gently vortexed, incubated for 15 min at 25 °C in the dark, and finally mixed with 400 μL of 1× binding buffer. The apoptotic cell population was determined on an Accuri C6 flow cytometer within 1 h. 10,000 cell events were counted for each sample. Unstained cells, and the cells stained with FITC Annexin V only and PI only, were used to set up compensation and quadrants. Data was analyzed by FlowJo (TreeStar, Ashland, OR, USA).

2.6. Western blot analysis

Western blot was used to assess the expression of Bcl-2, procaspase-9 and procaspase-3, γH2AX and acetyl histone 3 in BxPC-3 and its D5D-*KD* counterpart upon different treatments *in vitro* as described elsewhere [34–38]. For their expression *in vivo,* tumor tissues (~ 50–100 mg) were frozen in liquid nitrogen and crushed to a fine powder, then the protein was extracted using CelLytic™ lysis reagent. The same amount of protein from each sample was then loaded into 10% SDS-PAGE gels. The gels were run at a constant current of 30 mA for 1 h, and proteins were then transferred to nitrocellulose membranes at a constant voltage of 80 V for 2 h on ice. The membranes were incubated with primary antibodies overnight at 4 °C and with horseradish peroxidase-conjugated secondary antibody for 1 h at room temperature with continuous rocking. Then the membranes were incubated in ECL western blot substrates for 2 min, followed by exposure to X-ray film. Luminescent signals were captured on a Mini-Medical Automatic Film Processor (Imageworks).

2.7. Determination of DGLA/AA ratio and [PGE2]

The ω-6s accessible to COX-2-catalyzed peroxidation and the formed PGE2 in cells were quantified *via* LC/MS analysis as described elsewhere [33–38]. For the *in vivo* study, tumor tissues (~ 50–100 mg) were weighed, frozen in liquid nitrogen, and crushed to a fine powder. The powders were then mixed with water and methanol as well as internal standards (AA-d_8, DGLA-d_6, and PGE2-d_9), 5.0 μL each. The mixtures were vortexed for 1 min and set on ice for 30 min, followed by the same extraction procedures as described in the *in vitro* experiment [33–38].

The LC/MS system, consisting of an Agilent 1200 series HPLC system and an Agilent 6300 LC/MSD SL ion trap MS, was used to quantify the free ω-6s and PGs in cells and tumor samples [33–38]. For quantification, an internal standard curve was constructed from a series of mixtures consisting of DGLA, AA, and PGE2 standard solutions at various concentrations, and the internal standards DGLA-d_6, AA-d_8, and PGE2-d_9 at a constant concentration. The concentrations of fatty acids and PGE2 in the samples were calculated using the internal standard curve by comparing the ratios of the peak areas of the analytes to the peak areas of their corresponding internal standards. Note that the final concentrations of each analyte in every tumor sample were normalized to the same unit (μg/g).

2.8. GC/MS analysis of [8-HOA]

8-HOA produced from cells was quantified *via* GC/MS analysis as its derivative of pentafluorobenzyl bromide (PFB-Br) as described elsewhere [35–39]. In the *in vivo* study, tumor tissues (~ 50–100 mg) frozen in liquid nitrogen were crushed to a powder and suspended in 1.0 mL water. The suspension was mixed with 500 μL of methanol containing an internal standard (hexanoic acid), 50 μL of 1.0 N HCl, and 3.0 mL of dichloromethane, followed by the same procedures as the *in vitro* experiment.

Cell and tumor sample solutions (2.0 μL) were injected into an Agilent 7890 A gas chromatograph. The GC oven temperature was programmed from 60 to 300 °C at 25 °C/min. The injector and transfer line were kept at 280 °C. Quantitative analysis was performed using a mass selective detector with a source temperature of 230 °C. For quantification, an internal standard curve was constructed from a series of mixtures consisting of 8-HOA at various concentrations, and the internal standard hexanoic acid at a constant concentration. The concentrations of 8-HOA in the samples were calculated using the internal standard curve by comparing the ratios of the peak area of the 8-HOA to the peak area of the internal standard. The final concentrations of 8-HOA quantified in each tumor in the mice were normalized to the same unit (μg/g).

2.9. Immunofluorescence analysis

Expression of D5D, COX-2, cleaved PARP, Ki-67, MMP-2 and E-cadherin in tumor tissues was analyzed by immunofluorescence at the Advanced Imaging & Microscopy Laboratory, NDSU. Briefly, freshly collected tumor tissues were fixed with 10% formaldehyde and embedded in paraffin blocks. Tissue sections were deparaffinized with xylene, rinsed, and rehydrated through a graded series of alcohol. After antigen retrieval, the tumor sections were incubated with primary antibodies and subsequently with fluorochrome-conjugated secondary antibodies. Cell nuclei were counter-stained with DAPI. The images were acquired with a Zeiss Axio Imager M2 microscope.

Expression levels of D5D, COX-2, MMP-2, and E-cadherin in tumors were quantified *via* mean fluorescence intensities using Image Pro software (Media Cybernetics, Inc. Rockville, MD). The expression levels of cleaved PARP were presented as the percentage of cleaved PARP-positive cells *vs.* the total number of tumor cells. Similarly, the percentage of Ki-67-positive events relative to the total number of events was used for the quantification of the expression level of Ki-67.

2.10. Statistics

For the *in vitro* studies, data were presented as mean ± standard deviation (SD) from at least three separate experiments. For the *in vivo* study, data were presented as mean ± SD from six tumor samples per treatment group. Statistical differences between the mean values for different groups were evaluated by analysis of variance (ANOVA) and post hoc *t*-test; differences were considered significant with a p-value < 0.05.

3. Results

3.1. Inhibition of pancreatic cancer cell growth by promoted 8-HOA formation from DGLA

BxPC-3 is a human pancreatic carcinoma cell line with high COX-2 expression, thus is commonly used for COX-2 related cancer research [36,37,40]. We have previously reported that our novel anti-cancer concept (*i.e.*, considering high COX-2 to be a benefit for cancer cell killing, and the strategy of siRNA-D5D along with DGLA treatment) can successfully inhibit BxPC-3 cell growth, migration and invasion [36,37]. In this study, we created stable D5D-knockdown BxPC-3 (D5D-*KD* cells) *via* shRNA-transfection with a ~70% inhibited D5D expression compared to D5D-wild type BxPC-3 (*wt*-D5D cells, Fig. 1**A**). Consistent with our previous reports [36,37], 48 h treatment with 100 μM DGLA significantly increased the ratio of DGLA/AA in D5D-*KD* cells, as D5D controls the rate-limiting step that converts DGLA to AA. DGLA treatment also greatly promoted 8-HOA formation to a threshold level in D5D-*KD* cells (> 0.5 nmol/10^6 cells, dash line in Fig. 1**B,** [36,37]), whereas the 8-HOA level in *wt*-D5D cells was unable to reach the threshold level during a 48 h incubation due to the much lower ratio of

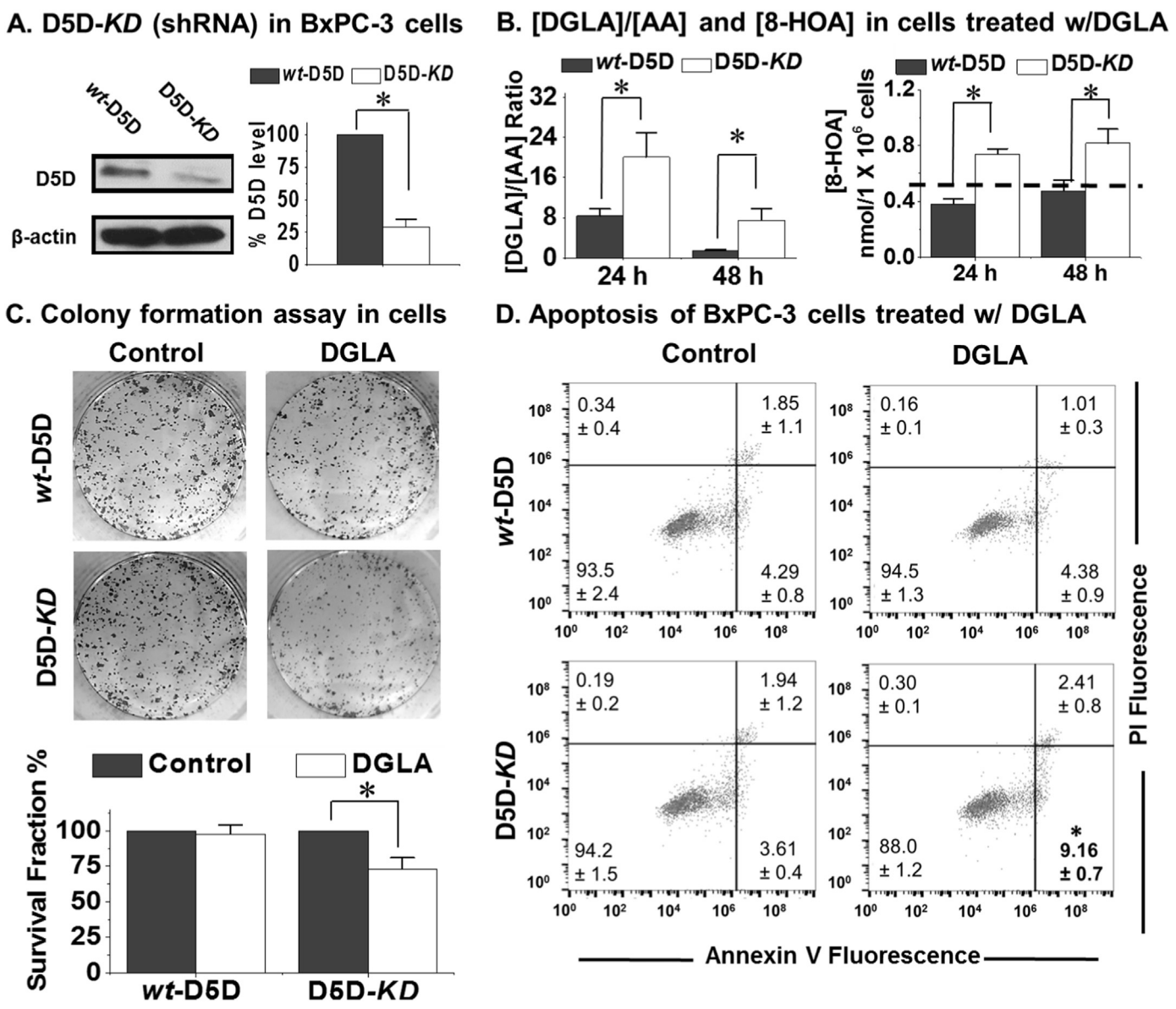

Fig. 1. D5D-*KD* and DGLA treatment promoted 8-HOA formation and inhibited BxPC-3 cell growth. **(A)** Western blot and relative expression level of D5D in *wt*-D5D and D5D-*KD* BxPC-3 cells (loading control: β-actin). The ratio of D5D to β-actin in the control was normalized; **(B)** Left: LC/MS quantification of DGLA/AA ratio from cell medium containing 1.0×10^6 of *wt*-D5D and D5D-*KD* BxPC-3 cells after DGLA treatment (100 μM), and Right: GC/MS quantification of 8-HOA from cell medium containing 1.0×10^6 of *wt*-D5D and D5D-*KD* BxPC-3 cells after DGLA treatment (100 μM). The dashed line indicates the threshold level of 8-HOA; **(C)** Colony formation and calculated survival fraction of *wt*-D5D and D5D-*KD* BxPC-3 cells 10 days after DGLA treatment (100 μM for 48 h). The survival fractions for control groups were normalized to 100%; and **(D)** Apoptosis analysis (Annexin V-FITC/PI double staining) of *wt*-D5D and D5D-*KD* BxPC-3 cells after DGLA treatment (100 μM for 48 h). All the quantification data represent mean ± SD with at least three separate experiments. *: significant difference *vs*. control with $p < 0.05$.

DGLA/AA available for COX-2 peroxidation.

The promoted 8-HOA from DGLA significantly inhibited colony formation in D5D-*KD* cells (the surviving fraction was 72.9% *vs.* 100% in control), but had no inhibitory effect on *wt*-D5D cells (surviving fraction 97.9%, Fig. 1**C**). Promoted formation of 8-HOA in D5D-*KD* cells also induced apoptosis, as demonstrated by annexin V-FITC/PI staining (population of early apoptotic cells 9.16% *vs.* 3.61% in the control, Fig. 1**D**), while no such effect was observed in *wt*-D5D cells with their low 8-HOA formation.

3.2. DGLA and D5D-KD enhanced gemcitabine's efficacy in BxPC-3 cells

Gemcitabine, a nucleoside analog, has been used as the most common chemotherapy drug to treat pancreatic cancer. However, resistance to gemcitabine has been a major obstacle for pancreatic cancer therapy. Here gemcitabine alone inhibited D5D-*KD* BxPC-3 cell growth with a survival fraction at 50.9% (*vs.* 100% in the control), while DGLA (100 μM) as a co-treatment, promoting 8-HOA formation, further increased gemcitabine's cytotoxicity to D5D-*KD* cells (survival fraction 32.4%, Fig. 2**A**). Gemcitabine treatment alone induced apoptosis in D5D-*KD* cells (population of early apoptotic cells 12.6% *vs.* 3.61% in control, Fig. 2**B**), while concurrent DGLA treatment (100 μM) further promoted gemcitabine-induced apoptosis in D5D-*KD* cells (17.2%). However, DGLA treatment had no influence on gemcitabine's cytotoxicity on *wt*-D5D cells as the threshold level of 8-HOA could not be reached (Fig. 1B).

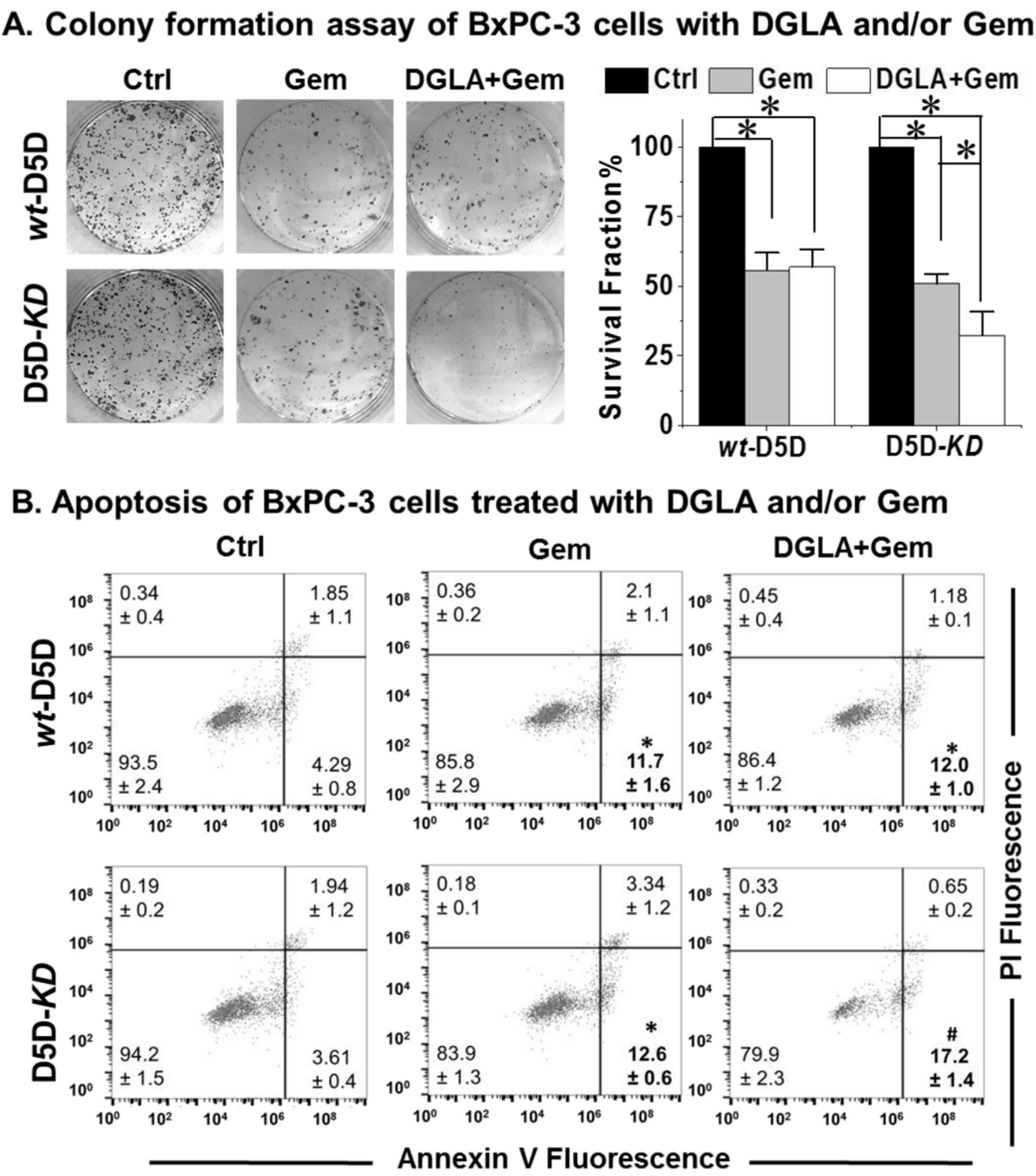

Fig. 2. Promoted 8-HOA formation improved gemcitabine's cytotoxicity in D5D-*KD* BxPC-3 cells. **(A)** Colony formation and calculated survival fraction of *wt*-D5D and D5D-*KD* BxPC-3 cells 10 days after DGLA (100 μM) and/or gemcitabine (0.1 μM) treatment. The survival fractions for control groups were normalized to 100% (*: significant difference with $p < 0.05$); **(B)** Apoptosis analysis (Annexin V-FITC/PI double staining) of *wt*-D5D and D5D-*KD* BxPC-3 cells at 48 h after DGLA (100 μM) and/or gemcitabine (0.1 μM) treatment (*: significant difference *vs.* control with $p < 0.05$, #: significant difference *vs.* gemcitabine treatment group with $p < 0.05$). All the quantification data represent mean ± SD with at least three separate experiments.

3.3. DGLA supplementation promoted 8-HOA formation in D5D-KD xenograft tumors

In order to investigate the anti-tumor effect from COX-2-catalyzed DGLA peroxidation, immuno-deficient mice were implanted with BxPC-3 cells or their D5D-*KD* counterpart, and subjected to 4-week treatments of vehicle control, DGLA ethyl ester, gemcitabine alone or a combination of DGLA ethyl ester and gemcitabine. Expression levels of

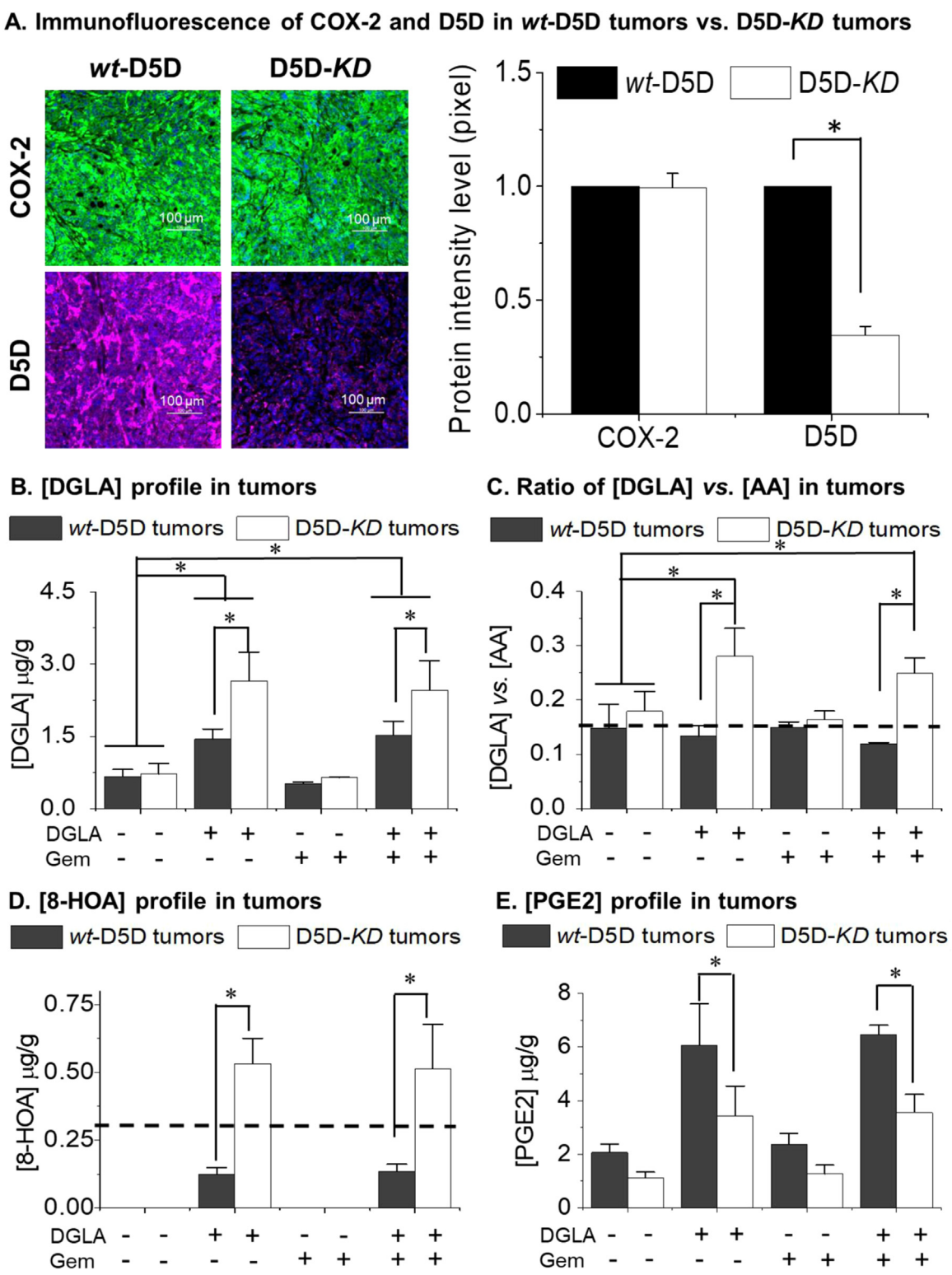

Fig. 3. D5D-*KD* suppressed DGLA conversion and promoted 8-HOA formation in tumors. **(A)** Left panel, representative immunofluorescence images for COX-2 and D5D expression in *wt*-D5D and D5D-*KD* tumor tissues; COX-2 was stained in green, D5D was stained in pink, cell nuclei were counterstained with DAPI. Right panel, mean intensity of COX-2 and D5D; **(B)** LC/MS quantification of DGLA levels from tumor tissues; **(C)** LC/MS quantification of DGLA/AA ratio from tumor tissues. The dashed line indicates the basal level of DGLA/AA in tumors without DGLA supplementation; **(D)** GC/MS quantification of 8-HOA from tumor tissues. The dashed line indicates the threshold level of 8-HOA in D5D-*KD* tumors; and **(E)** LC/MS quantification of PGE2 from tumor tissue. All the quantification data represent mean ± SD with six tumor samples. *: significant difference with $p < 0.05$.

D5D in tumor tissues of the mice after different treatments were assessed by immunofluorescence in order to confirm shRNA-knockdown efficiency. Regardless of treatment, D5D-*KD* tumors had significantly lower D5D expression than *wt*-D5D tumors (Fig. 3**A**). COX-2 levels in all tumors were also assessed, and D5D-*KD* and all other treatments had no influence on the COX-2 levels (Fig. 3A).

The levels of DGLA and the ratio of DGLA/AA in tumors from experimental animals were measured by HPLC/MS. Without DGLA supplementation, there was no difference in DGLA levels or DGLA/AA ratios in tumors between the vehicle control and gemcitabine treatment groups; only basal levels of DGLA (~ 0.5–0.7 μg/g, Fig. 3**B**) and DGLA/AA (~ 0.15–0.18, Fig. 3**C**) formed in tumors from both control and gemcitabine treatment groups.

In the mice that had 4 weeks of DGLA supplementation, the DGLA level significantly increased (~ 1.4–1.5 μg/g, Fig. 3B) in *wt*-D5D tumors, while the DGLA/AA ratio remained similar to the basal level (~ 0.12–0.13, Fig. 3C). The effective conversion of DGLA to AA in *wt*-D5D tumors is responsible for the unchanged ratio of DGLA/AA in mice with DGLA supplementation. On the other hand, in D5D-*KD* tumors from mice with 4 weeks of DGLA supplementation, not only was the DGLA level greatly elevated (~ 2.4–2.6 μg/g, Fig. 3B), but also the ratio of DGLA/AA increased significantly compared to all other groups (~ 0.25–0.28, dash line in Fig. 3C).

Consistently, in the mice without DGLA supplementation, only basal levels of 8-HOA were formed in both *wt*-D5D and D5D-*KD* tumors (under the detection limit, Fig. 3**D**). However, there were significantly increased levels of 8-HOA (~ 0.5 μg/g) in D5D-*KD* tumors *vs.* *wt*-D5D tumors (< 0.14 μg/g, Fig. 3D) from the mice with DGLA supplementation. Although DGLA supplementation also increased the level of PGE2 in all tumors, much lower amounts of PGE2 were detected in D5D-*KD* tumors than in *wt*-D5D tumors (~ 3.4 *vs.* ~ 6.1 μg/g, Fig. 3**E**). Since both ω-6s are COX-2 substrates, the DGLA/AA ratio is more critical than the absolute DGLA level in ensuring that ω-6s are metabolized in tumors in a way that reaches a threshold level of 8-HOA (~ 0.3 μg/g, dashed line in Fig. 3D) for executing its anti-cancer effects.

3.4. Inhibition of D5D-KD xenograft tumor growth by promoted formation of 8-HOA

The tumor sizes of experimental animals were measured twice a week. Four weeks of DGLA supplementation did not affect the growth of *wt*-D5D tumors (Fig. 4**A**), consistent with the low level of 8-HOA in *wt*-D5D tumors (Fig. 3D). On the other hand, DGLA supplementation resulted in significantly reduced tumor size and growth rate (Fig. 4**B**), associated with the formation of 8-HOA at greater than the threshold level in D5D-*KD* tumors. About a 30% reduction of D5D-*KD* tumors in mice fed a diet with DGLA supplementation was achieved compared to the *wt*-D5D tumor control group (Fig. 4A).

Gemcitabine inhibited tumor growth in both the *wt*-D5D group and the D5D-*KD* group (Fig. 4A-B), while DGLA supplementation only affected the D5D-*KD* tumor size (~ 90.2 ± 43.1 mm^3, Fig. 4B), giving similar or slightly improved anti-tumor effects *vs.* gemcitabine treatment for *wt*-D5D tumors (~86.9 ± 34.4 mm^3, Fig. 4A). Co-treatment with DGLA and gemcitabine led to a greater reduction in D5D-*KD* tumors (37.7 ± 20.4 mm^3, Fig. 4B).

3.5. Effect of D5D-KD and DGLA supplementation in tumor proliferation and apoptosis

Immunofluorescence studies were also conducted to test whether our strategy could inhibit tumor proliferation and induce apoptosis. DGLA supplementation did not have any influence on the expression of Ki-67 (proliferation marker) in *wt*-D5D tumors compared to the control group, whereas treatment with gemcitabine as well as the combination of gemcitabine and DGLA supplementation led to significantly less expression of Ki-67 (Fig. 5**A**). On the other hand, DGLA supplementation

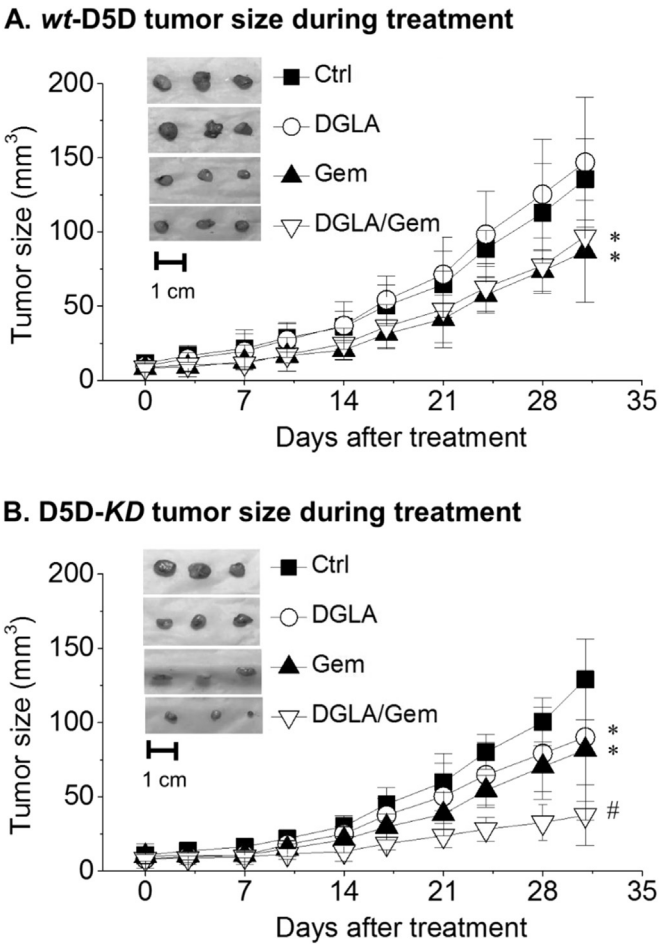

Fig. 4. Effect of DGLA supplementation on BxPC-3 xenograft tumor growth. **(A)** Measured *wt*-D5D tumor size during the 4-week treatment (vehicle control, DGLA, gemcitabine, or DGLA + gemcitabine, 6 mice per treatment group) and photos of tumor tissues at the end of the treatment; **(B)** Measured D5D-*KD* tumor size during the 4-week treatment and photos of tumor tissues at the end of the treatment. *: significant difference *vs.* corresponding control with $p < 0.05$, #: significant difference *vs.* single treatment with $p < 0.05$.

resulted in significantly decreased expression of Ki-67 in D5D-*KD* tumors compared to the vehicle control (*i.e.*, the percentage of Ki-67 positive cells, ~ 58.1% *vs.* 80.6%). In addition, while gemcitabine alone suppressed tumor proliferation, the combination of DGLA supplementation and gemcitabine in D5D-*KD* tumors resulted in even less expression of Ki-67.

The expression of cleaved PARP (tumor apoptotic marker) was examined by immunofluorescence analysis as well. In *wt*-D5D tumors, DGLA supplementation did not induce apoptosis, thus gemcitabine and the combination (gemcitabine and DGLA supplementation) led to similar levels of tumor apoptosis (Fig. 5**B**). On the other hand, for D5D-*KD* tumors, DGLA supplementation induced apoptosis to a level similar to that of gemcitabine treatment. The combination of DGLA supplementation and gemcitabine resulted in even more apoptosis in D5D-*KD* tumors (Fig. 5B).

We also conducted western blotting to investigate the molecular mechanisms. In *wt*-D5D tumors, DGLA supplementation had no effect on expression of apoptotic proteins or acetyl histone H3 (Fig. 5**C**). However, in D5D-*KD* tumors, DGLA supplementation resulted in significantly decreased expressions of Bcl-2 (anti-apoptotic protein), procaspase-9 and procaspase-3, representing activation of the p53-independent cell/tumor apoptotic pathway (Fig. 5C). DGLA supplementation also resulted in accumulation of acetyl histone H3 and γH2AX in D5D-*KD* tumors, which is consistent with our previous *in vitro*

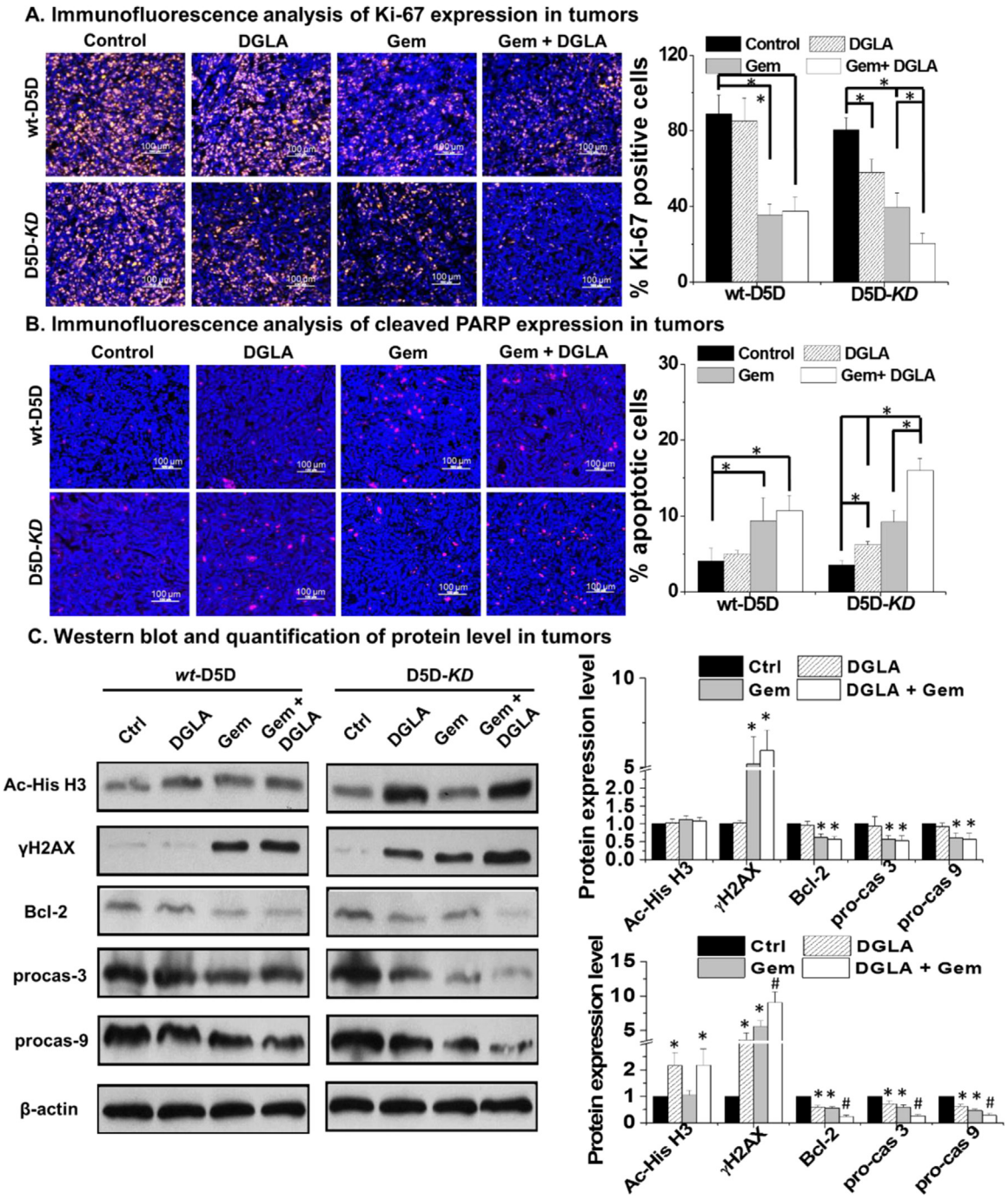

Fig. 5. Effect of D5D-*KD* and DGLA in BxPC-3 xenograft tumor proliferation and apoptosis. **(A)** Representative images and quantification for Ki-67 expression in tumor tissues. Ki-67 were stained in yellow, cell nuclei were counterstained with DAPI; **(B)** Representative images and quantification for cleaved PARP expression in tumor tissues. Cleaved PARP expression was stained in red, and cell nuclei were counterstained with DAPI; and **(C)** Western blot and relative protein expression levels of bcl-2, procaspase 3, procaspase 9, acetyl histone H3 and γH2AX in tumor tissues. β-actin served as a loading control. The ratio of each protein to β-actin in the controls was normalized to 1. All the quantification data represent mean ± SD with six tumor samples. *: significant difference *vs.* control with $p < 0.05$.

experiments [36,37]. Our studies confirmed that the promoted formation of 8-HOA in D5D-*KD* cells could suppress cancer cell/tumor growth *via* inhibiting HDAC and damaging DNA. In comparison, in *wt*-D5D tumors, DGLA supplementation alone failed to activate apoptosis, with no changed HDAC activity, as 8-HOA never reached the threshold level.

3.6. DGLA supplementation suppressed metastasis potential in D5D-KD tumors

Previous studies have demonstrated that D5D-*KD* and DGLA can suppress cancer cell migration and invasion in BxPC-3 cells. Here the tumors from the *wt*-D5D and D5D-*KD* groups were tested *via* immunofluorescence for expression of protein markers that play important roles in cancer metastasis. DGLA supplementation had no influence on the expression of MMP-2 (marker for tumor metastasis) in *wt*-D5D tumor tissues compared to the control group. However, DGLA supplementation resulted in a significantly increased expression of MMP-2 in D5D-*KD* tumors *vs*. the vehicle control (Fig. 6**A**). Further decreased expression of MMP-2 was observed in D5D-*KD* tumors treated with the combination of DGLA and gemcitabine, while in *wt*-D5D tumors, the

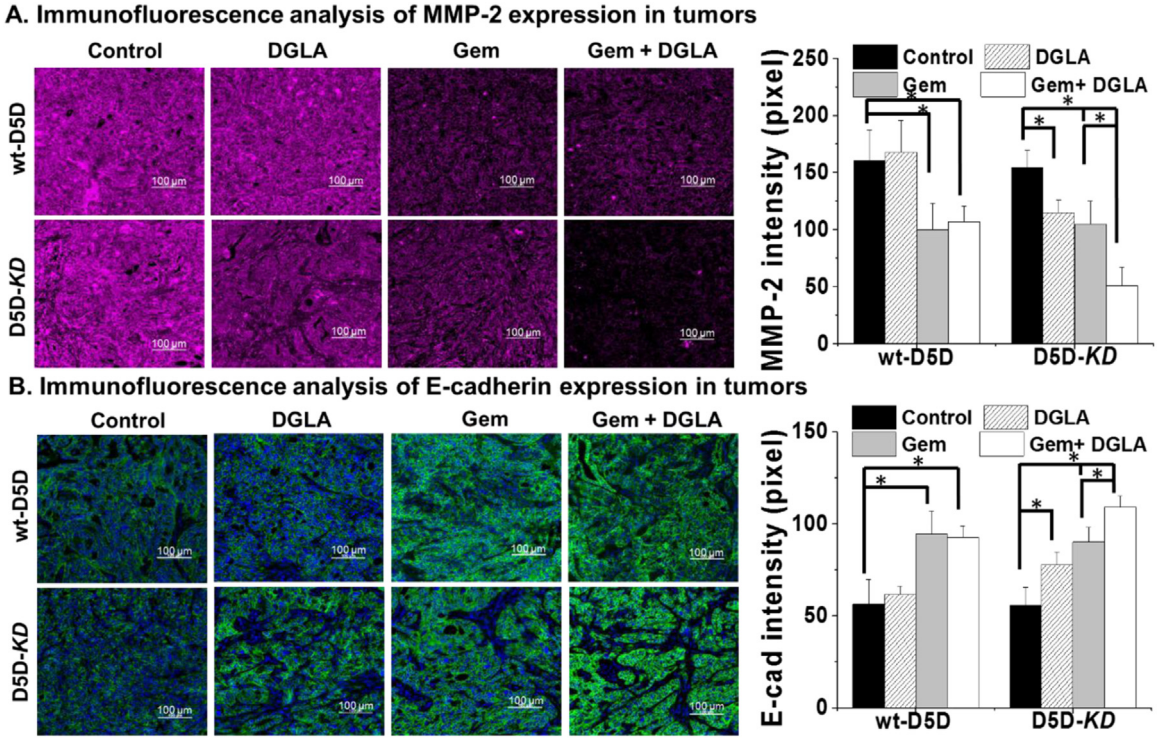

Fig. 6. Immunofluorescence analysis of MMP-2 and E-cadherin expression in tumor tissues. **(A)** Representative images and quantification for MMP-2 expression in tumor tissues. MMP-2 were stained in red, cell nuclei were counterstained with DAPI; **(B)** Representative images and quantification for E-cadherin expression in tumor tissues. E-cadherin were stained in green, and cell nuclei were counterstained with DAPI. All the quantification data represent mean ± SD with six tumor samples. *: significant difference with $p < 0.05$.

combination did not further downregulate MMP-2 expression.

DGLA supplementation did not alter the level of E-cadherin in *wt*-D5D tumors, while in D5D-*KD* tumors, DGLA supplementation significantly upregulated expression of E-cadherin (Fig. 6**B**). Further increased expression of E-cadherin was observed in D5D-*KD* tumors co-treated with DGLA and gemcitabine, while in *wt*-D5D tumors, the combination did not further upregulate E-cadherin.

4. Discussion

There is currently no cure for pancreatic cancer as it is hard to detect at early stage, usually not treatable by surgery and radiation, and resistant to chemotherapy drugs. We previously reported that DGLA treatment along with D5D knockdown in various types of cancer cell lines (including pancreatic cancer) led to promoted formation of 8-HOA (an HDAC inhibitor) from COX-2-catalyzed DGLA peroxidation, which in turn inhibited cancer cell growth, migration, and invasion [36,37]. In this study, we further investigated the anti-tumor effect of D5D-*KD* combined with a DGLA supplementation strategy, as well as the novel COX-2 biology concept, in xenograft tumors bearing shRNA-transfected BxPC-3 cells targeting D5D.

Consistent with previous *in vitro* experiments [36,37], we observed that DGLA treatment inhibited the growth of D5D-*KD* cells by promoting the formation of 8-HOA at a threshold level (Fig. 1), and significantly improved the efficacy of gemcitabine (Fig. 2). Similarly, DGLA supplementation promoted the formation of 8-HOA to a threshold level in D5D-*KD* tumors and maintained a higher DGLA/AA ratio for COX-2-catalyzed peroxidation. The ratio seems to be more important than the actual DGLA level for formation of a threshold level of 8-HOA in tumors (Fig. 3) as both DGLA and AA are COX-2 substrates. DGLA supplementation resulted in the formation of a high level of 8-HOA in an autocrine manner in D5D-*KD* tumors, consequently inhibiting their growth (Fig. 4).

We also observed that gemcitabine treatment alone significantly inhibited the growth of both *wt*-D5D and D5D-*KD* tumors (Fig. 4). In *wt*-D5D tumors, concurrent DGLA supplementation and gemcitabine had no improved anti-cancer effects beyond that of gemcitabine alone (Fig. 4). A two-factor analysis considering gemcitabine and D5D-*KD*/DGLA as the factors (Supplemental Table 1) was conducted for following four groups: *wt*-D5D tumors vehicle control; *wt*-D5D tumors with gemcitabine only; D5D-*KD* tumors with DGLA supplementation; and D5D-*KD* tumors with a combination of DGLA supplementation and gemcitabine. An additive effect on tumor reduction from the combination was achieved (70% *vs.* *wt*-D5D tumors). As HDAC inhibitors have been reported to be able to synergistically enhance the anti-cancer activities of various chemo- and targeted-cancer drugs [41,42], we also plan to combine our new anti-cancer strategy with different anti-cancer reagents for achieving synergistic improvement with 8-HOA. Unlike chemotherapy, which commonly causes drug resistance and/or drug-related toxicity issues, the dosage and duration of DGLA supplementation in our strategy could be readily adjusted and optimized to form the anti-cancer product 8-HOA in an autocrine manner in tumors in order to pursue a safer and better tumor reduction outcome.

The body weight of the mice was also monitored throughout the experiment (Supplemental Fig. 1). There is no severe toxicity observed from our treatment strategy, as no significant change in body weight was observed among the different groups during the four-week treatment period.

MMP-2 is a protein able to degrade the extracellular matrix in cancer progression, which allows cancer cells to migrate and invade from the primary tumor site. In D5D-*KD* tumors, DGLA supplementation significantly inhibited MMP-2 expression, consistent with the associated high level of 8-HOA but low level of PGE2 (Fig. 3). E-cadherin plays an important role in epithelial cell adhesion. Down-regulation of E-cadherin expression was observed in the tumor environment, correlating with a strong invasive potential [43]. DGLA supplementation result in a significantly increased level of E-cadherin in D5D-*KD* tumors compared to the vehicle control (Fig. 6). We have not observed

metastasizing tumors anywhere in our xenograft study under the current treatments. Orthotopic tumor models have been already established in our lab for investigating whether spontaneous metastasis can be inhibited by our strategy.

Delivery of therapeutic RNAs to tumors has remained a difficult task due to stability issues of the siRNA products, safety concerns for shRNA vectors, and many other limitations [44]. Therefore, we are now working on employing innovative nano-carriers for specifically delivering D5D-targeting siRNA into pancreatic cancer cells [45]. In addition, instead of using siRNA, we have identified a lead compound as a D5D inhibitor and confirmed that it is much better than many commercial D5D inhibitor molecules not only for inhibiting DGLA to AA, but also showing much greater anti-cancer activity *in vitro* and *in vivo* when concurrently used with DGLA supplementation. In addition, we also designed and synthesized several derivatives based on the lead compound which showed even more potent D5D inhibitory effects. Unfortunately, we are not allowed to release the compound structure and our research data, as we just converted our method/compound from US-provisional patent to a US patent.

In conclusion, our research shows that DGLA supplementation in D5D-*KD* tumors promotes 8-HOA formation from COX-2 catalyzed peroxidation, which in turn regulates histone deacetylation and induces DNA damage, thereby triggering the activation of the cell apoptosis pathway, and leads to inhibition of pancreatic tumor growth. Instead of inhibiting COX-2, we can now take advantage of the high COX-2 expression in cancer cells to promote the formation of the anti-cancer byproduct 8-HOA to suppress pancreatic cancer development. We believe that this novel strategy will lead to better therapeutic effects in pancreatic cancer treatment due to its dual anti-cancer mechanisms, *i.e.*, promoting the anti-cancer effect from DGLA while limiting the pro-cancer effect from AA. Our strategy will also be expected to have fewer side effects and safer cancer treatment outcomes, as cancers in general have overexpressed COX-2 levels and much higher fatty acid intake rates than normal cells and tissues [14–16,46]. In addition, our proposed strategy of making use of this hallmark of cancer cells to work against the cancer cell itself would provide an excitingly novel insight into cancer therapy and challenge the current paradigm of COX-2 biology in cancer treatment.

Acknowledgement

This work was supported by National Cancer Institute (R15CA195499), National Institute of General Medical Sciences (P20GM109024), and Sanford Health-NDSU Seed Grant (FAR0026507).

Author contribution

Xiaoyu Yang and Yi Xu for investigation, methodology, writing original draft; Di Gao for formal analysis; Liu Yang for conceptualization, review and editing; Steven Qian for conceptualization, funding acquisition, supervision and review and editing.

Conflict of interest

The authors declare no conflict of interest

Appendix A. Supplementary material

Supplementary data associated with this article can be found in the online version at doi:10.1016/j.redox.2018.10.001.

References

[1] A. Mohammed, N.B. Janakiram, M. Brewer, A. Duff, S. Lightfoot, R.S. Brush, R.E. Anderson, C.V. Rao, Endogenous n-3 polyunsaturated fatty acids delay progression of pancreatic ductal adenocarcinoma in fat-1-p48(Cre/þ)-LSL-Kras (G12D/+) mice, Neoplasia 14 (2012) 1249–1259.
[2] M. Fukui, K.S. Kang, K. Okada, B.T. Zhu, EPA, an omega-3 fatty acid, induces apoptosis in human pancreatic cancer cells: role of ROS accumulation, caspase-8 activation, and autophagy induction, J. Cell. Biochem. 114 (2013) 192–203.
[3] K.S. Song, K. Jing, J.S. Kim, E.J. Yun, S. Shin, K.S. Seo, J.H. Park, J.Y. Heo, J.X. Kang, K.S. Suh, T. Wu, J.I. Park, G.R. Kweon, W.H. Yoon, B.D. Hwang, K. Lim, Omega-3-polyunsaturated fatty acids suppress pancreatic cancer cell growth in vitro and in vivo via downregulation of Wnt/Beta-catenin signaling, Pancreatology 11 (2011) 574–584.
[4] T. Shirota, S. Haji, M. Yamasaki, T. Iwasaki, T. Hidaka, Y. Takeyama, H. Shiozaki, H. Ohyanagi, Apoptosis in human pancreatic cancer cells induced by eicosa-pentaenoic acid, Nutrition 21 (2005) 1010–1017.
[5] N. Merendino, B. Loppi, M.D. Aquino, R. Molinari, G. Pessina, C. Romano, F. Velotti, Docosahexaenoic acid induces apoptosis in the human PaCa-44 pancreatic cancer cell line by active reduced glutathione extrusion and lipid peroxidation, Nutr. Cancer 52 (2005) 225–233.
[6] D. D'Eliseo, L. Manzi, N. Merendino, F. Velotti, Docosahexaenoic acid inhibits invasion of human RT112 urinary bladder and PT45 pancreatic carcinoma cells via down-modulation of granzyme B expression, J. Nutr. Biochem. 23 (2012) 452–457.
[7] N. Merendino, R. Molinari, B. Loppi, G. Pessina, M.D. Aquino, G. Tomassi, F. Velotti, Induction of apoptosis in human pancreatic cancer cells by docosahexaenoic acid, Ann. N. Y. Acad. Sci. 1010 (2003) 361–364.
[8] K.S. Park, J.W. Lim, H. Kim, Inhibitory mechanism of omega-3 fatty acids in pancreatic inflammation andapoptosis, Ann. N. Y. Acad. Sci. 1171 (2009) 421–427.
[9] J. Haqq, L.H. Howells, G. Garcea, A.R. Dennison, Targeting pancreatic cancer using a combination of gemcitabine with the omega-3 polyunsaturated fatty acid emulsion, Lipidem™, Mol. Nutr. Food. 60 (2016) 1437–1447.
[10] J. Hering, S. Garrean, T.R. Dekoj, A. Razzak, A. Saied, J. Trevino, T.A. Babcock, N.J. Espat, Inhibition of proliferation by omega-3 fatty acids in chemoresistant pancreatic cancer cells, Ann. Surg. Oncol. 14 (2007) 3620–3628.
[11] A.P. Simopoulos, A. Leaf, N. Salem Jr., Essentiality of and recommended dietary intakes for omega-6 and omega-3 fatty acids, Ann. Nutr. Metab. 43 (1999) 127–130.
[12] R.A. Woutersen, M.J. Appel, A. van Garderen-Hoetmer, M.V. Wijnands, Dietary fat and carcinogenesis, Mutat. Res. 443 (1999) 111–127.
[13] P.C. Calder, Dietary modification of inflammation with lipids, Proc. Nutr. Soc. 61 (2002) 345–358.
[14] C.E. Eberhart, R.J. Coffey, A. Radhika, F.M. Giardiello, S. Ferrenbach, R.N. DuBois, Up-regulation of cyclooxygenase 2 gene expression in human colorectal adenomas and adenocarcinomas, Gastroenterology 107 (1994) 1183–1188.
[15] X. Ma, T. Aoki, T. Tsuruyama, S. Narumiya, Definition of prostaglandin E2-EP2 signals in the colon tumor microenvironment that amplify inflammation and tumor growth, Cancer Res. 75 (2015) 2822–2832.
[16] S. Ogino, G.J. Kirkner, K. Nosho, N. Irahara, S. Kure, K. Shima, A. Hazra, A.T. Chan, R. Dehari, E.L. Giovannucci, C.S. Fuchs, Cyclooxygenase-2 expression is an independent predictor of poor prognosis in colon cancer, Clin. Cancer Res. 14 (2008) 8221–8227.
[17] C.A. Rouzer, L.J. Marnett, Endocannabinoid oxygenation by cyclooxygenases, lipoxygenases, and cytochromes P450: cross-talk between the eicosanoid and endocannabinoid signaling pathways, Chem. Rev. 111 (2011) 5899–5921.
[18] E. Granstrom, The arachidonic acid cascade. The prostaglandins, thromboxanes and leukotrienes, Inflammation 8 (1984) S15–S25.
[19] D. Wang, R.N. Dubois, The role of COX-2 in intestinal inflammation and colorectal cancer, Oncogene 29 (2010) 781–788.
[20] W.L. Smith, I. Song, The enzymology of prostaglandin endoperoxide H synthases-1 and -2, Pros. Other Lipid Med. 68–69 (2002) 115–128.
[21] W.L. Smith, R.M. Garavito, D.L. DeWitt, Prostaglandin endoperoxide H synthases (cyclooxygenases)-1 and -2, J. Biol. Chem. 271 (1996) 33157–33160.
[22] W.L. Smith, Y. Urade, P.J. Jakobsson, Enzymes of the cyclooxygenase pathways of prostanoid biosynthesis, Chem. Rev. 111 (2011) 5821–5865.
[23] M.T. Yip-Schneider, D.S. Barnard, S.D. Billings, L. Cheng, D.K. Heilman, A. Lin, S.J. Marshall, P.L. Crowell, M.S. Marshall, C.J. Sweeney, Cyclooxygenase-2 expression in human pancreatic adenocarcinomas, Carcinogenesis 21 (2000) 139–146.
[24] A. Kirane, J.E. Toombs, K. Ostapoff, J.G. Carbon, S. Zaknoen, J. Braunfeld, R.E. Schwarz, F.J. Burrows, R.A. Brekken, Apricoxib, a novel inhibitor of COX-2, markedly improves standard therapy response in molecularly defined models of pancreatic cancer, Clin. Cancer Res. 18 (2012) 5031–5042.
[25] H.A. Al-Wadei, M.H. Al-Wadei, M.F. Ullah, H.M. Schuller, Celecoxib and GABA cooperatively prevent the progression of pancreatic cancer in vitro and in xenograft models of stress-free and stress-exposed mice, PLoS One 7 (2012) e43376.
[26] A. Lipton, C. Campbell-Baird, L. Witters, H. Harvey, S. Ali, PhaseII trial of gemcitabine, irinotecan, and celecoxib in patients with advanced pancreatic cancer, J. Clin. Gastroenterol. 44 (2010) 286–288.
[27] N. Ding, X.X. Cui, Z. Gao, H. Huang, X. Wei, Z. Du, Y. Lin, W.J. Shih, A.B. Rabson, A.H. Conney, C. Hu, X. Zheng, A triple combination of atorvastatin, celecoxib and tipifarnib strongly inhibits pancreatic cancer cells and xenograft pancreatic tumors, Int. J. Oncol. 44 (2014) 2139–2145.
[28] M.A. Molina, M. Sitja-Arnau, M.G. Lemoine, M.L. Frazier, F.A. Sinicrope, In-creased cyclooxygenase-2 expression in human pancreatic carcinomas and cell lines: growth inhibition by nonsteroidal anti-inflammatory drugs, Cancer Res. 59 (1999) 4356–4362.
[29] H. Yokouchi, K. Kanazawa, Revisiting the role of COX-2 inhibitor for non-small cell lung cancer, Transl. Lung Cancer Res. 4 (2015) 660–664.
[30] R.S. Bresalier, R.S. Sandler, H. Quan, J.A. Bolognese, B. Oxenius, K. Horgan, C. Lines, R. Riddell, D. Morton, A. Lanas, M.A. Konstam, J.A. BaronAdenomatous Polyp Prevention on Vioxx (APPROVe) Trial Investigators, Cardiovascular events

associated with rofecoxib in a colorectal adenoma chemoprevention trial, N. Engl. J. Med. 352 (2005) 1092–1102.
[31] C. Sostres, C.J. Gargallo, M.T. Arroyo, A. Lanas, Adverse effects of non-steroidal anti-inflammatory drugs (NSAIDs, aspirin and coxibs) on upper gastrointestinal tract, Best. Pract. Res. Clin. Gastroenterol. 24 (2010) 121–132.
[32] C. Scarpignato, R.H. Hunt, Nonsteroidal antiinflammatory drug-related injury to the gastrointestinal tract: clinical picture, pathogenesis, and prevention, Gastroenterol. Clin. North Am. 39 (2010) 433–464.
[33] Y. Gu, Y. Xu, B. Law, S.Y. Qian, The first characterization of free radicals formed from cellular COX-catalyzed peroxidation, Free Radic. Biol. Med. 57 (2013) 49–60.
[34] Y. Xu, J. Qi, X.Y. Yang, E. Wu, S.Y. Qian, Free radical derivatives formed from COX-catalyzed DGLA peroxidation can attenuate colon cancer cell growth and enhance 5-FU's cytotoxicity, Redox Biol. 2 (2014) 610–618.
[35] Y. Xu, X.Y. Yang, P.J. Zhao, Z.Y. Yang, C.H. Yan, B. Guo, S.Y. Qian, Knockdown of delta-5-desaturase promotes the anti-cancer activity of dihomo-γ-linolenic acid and enhances the efficacy of chemotherapy in colon cancer cells expressing COX-2, Free Radic. Biol. Med. 96 (2016) 67–77.
[36] X. Yang, Y. Xu, T. Wang, D. Shu, P. Guo, K.W. Miskimins, S.Y. Qian, Inhibition of cancer migration and invasion by knocking down delta-5-desaturase in COX-2 overexpressed cancer cells, Redox Biol. 11 (2017) 653–662.
[37] X. Yang, Y. Xu, A. Brooks, B. Guo, K.W. Miskimins, S.Y. Qian, Knockdown delta-5-desaturase promotes the formation of a novel free radical byproduct from COX-catalyzed ω-6 peroxidation to induce apoptosis and sensitize pancreatic cancer cells to chemotherapy drugs, Free Radic. Biol. Med. 97 (2016) 342–350.
[38] Y. Xu, X. Yang, W. Wang, L. Yang, Y. He, K. Miskimins, S.Y. Qian, Knockdown delta-5-desaturase in breast cancer cells that overexpress COX-2 results in inhibition of growth, migration and invasion via a dihomo-γ-linolenic acid peroxidation dependent mechanism, BMC Cancer 18 (2018) 330.
[39] O. Quehenberger, A. Armando, D. Dumlao, D.L. Stephens, E.A. Dennis, Lipidomics analysis of essential fatty acids in macrophages, Prostaglandins Leukot. Essent. Fat. Acids 79 (2008) 123–129.
[40] M.T. Yip-Schneider, D.S. Barnard, S.D. Billings, L. Cheng, D.K. Heilman, A. Lin, S.J. Marshall, P.L. Crowell, M.S. Marshall, C.J. Sweeney, Cyclooxygenase-2 expression in human pancreatic adenocarcinomas, Carcinogenesis 21 (2000) 139–146.
[41] M. Kalac, L. Scotto, E. Marchi, J. Amengual, V.E. Seshan, G. Bhagat, N. Ulahannan, V.V. Leshchenko, A.M. Temkin, S. Parekh, B. Tycko, O.A. O'Connor, HDAC inhibitors and decitabine are highly synergistic and associated with unique gene-expression and epigenetic profiles in models of DLBCL, Blood 118 (2011) 5506–5516.
[42] C.H. Chen, M.C. Chen, J.C. Wang, A.C. Tsai, C.S. Chen, J.P. Liou, S.L. Pan, C.M. Teng, Synergistic interaction between the HDAC inhibitor, MPT0E028, and sorafenib in liver cancer cells in vitro and in vivo, Clin. Cancer Res. 20 (2014) 1274–1287.
[43] E. Tsanou, D. Peschos, A. Batistatou, A. Charalabopoulos, K. Charalabopoulos, The E-cadherin adhesion molecule and colorectal cancer. A global literature approach, Anticancer Res. 28 (2008) 3815–3826.
[44] J.K.W. Lam, M.Y.T. Chow, Y. Zhang, S.W.S. Leung, siRNA versus miRNA as therapeutics for gene silencing, Mol. Ther. Nucleic Acids 4 (2015) e252.
[45] Y. Shu, H. Yin, M. Rajabi, H. Li, M. Vieweger, S. Guo, D. Shu, P. Guo, RNA-based micelles: a novel platform for paclitaxel loading and delivery, J. Control Release 276 (2018) 17–29.
[46] E. Currie, A. Schulze, R. Zechner, T.C. Walther, R.V. Farese, Cellular fatty acid metabolism and cancer, Cell Metab. 18 (2013) 153–161.